Dyes and Pigments 92 (2011) 573–579

Contents lists available at ScienceDirect

Dyes and Pigments

journal homepage: www.elsevier.com/locate/dyepig

Synthesis, optical properties and ultrafast dynamics of a 2,1,3-benzothiadiazole-based red emitter with intense fluorescence and large two-photon absorption cross-section

Yaochuan Wang [a,b], Ju Huang [c], Hui Zhou [a], Guohong Ma [d], Shixiong Qian [a,*], Xu-hui Zhu [c,**]

[a] Surface Physics Laboratory (State Key Laboratory), Physics Department, Fudan University, Shanghai 200433, People's Republic of China
[b] State Key Laboratory of Catalysis, Dalian Institute of Chemical Physics, Chinese Academy of Sciences, Dalian 116023, China
[c] State Key Laboratory of Physics and Chemistry of Luminescence and Institute of Polymer Optoelectronic Materials and Devices, South China University of Technology (SCUT), Guangzhou 510640, People's Republic of China
[d] Physics Department, Shanghai University, Shanghai 200000, People's Republic of China

ARTICLE INFO

Article history:
Received 31 October 2010
Received in revised form
25 June 2011
Accepted 27 June 2011
Available online 3 July 2011

Keywords:
Two-photon absorption
Two-photon fluorescence
Excited state dynamics
Intramolecular charge transfer
Benzothiadiazole
Red emitter

ABSTRACT

A new 2,1,3-benzothiadiazole-based red fluorescent compound with a D–A–D type structure was synthesized and characterized. The central 2,1,3-benzothiadiazole core was symmetrically connected via the 4,7-positions with two donor groups in which the 7-position of a fluorenyl ring was substituted with a carbazol-9-yl moiety and the 2-position was substituted by a 5-thienyl moiety. The carbazol moieties were further derivatized by two 2-naphthyl moieties at the 3,6-positions. Femtosecond laser spectroscopic techniques including excited state fluorescence and pump-probe technique investigations, together with steady state absorption and one-photon fluorescence spectra, were employed to systematically investigate the optical properties and ultrafast dynamics of the new compound in tetrahydrofuran solution. It shows a large two-photon absorption cross-section and high fluorescence quantum yield, indicating potential application in two-photon fluorescence imaging field. The ultrafast dynamics results reveal competition between a pure excited state relaxation process and stimulated radiation in the red wavelength region.

1. Introduction

Materials with large two-photon absorption (TPA) properties find a wide range of potential applications such as two-photon fluorescence (TPF) imaging, optical limiting, optical data storage, phototherapy and up-conversion lasing [1–6]. Among them, TPF imaging, which is usually under the excitation of picosend/femtosecond pulses in the near infrared region, makes possible fluosescence images of living cells, biological tissue and other objects with high three-dimensional spatial resolution, reduced photodamage and low background fluorescence interference [7]. However, the commonly used fluorophores are mainly blue or green emitters. Until now, investigations focused on the design and synthesis of efficient red emitters are quite limited [8–12], and their applications are restricted by small TPA cross-sections or low fluorescence quantum yields. The scarcity of excellent fluorophores showing a large TPA cross-section and efficient TPF emission in 600 ~ 800 nm wavelength region, a window widely recognized as being attractive for bio-analysis and *in-vivo* imaging, has become one of the major obstacles for these applications [13,14].

The 2,1,3-benzothiadiazole unit has been shown to be a convenient electron acceptor and used to construct π-conjugated functional organic materials in organic optoelectronic devices [15–22]. However, there are few reports about TPA materials using 2,1,3-benzothiadiazole as an electron acceptor [10–12]. The TPA applications will greatly benefit from large TPA cross-section and excellent fluorescent properties of the active compound. Various strategies for the design and synthesis of highly efficient two-photon active compounds have been proposed by manipulating electron donor (D) and/or acceptor (A) properties and their incorporation in a molecular architecture [23–26]. Two-photon excited fluorescence, Z-scan, degenerate four-wave mixing technique and many other techniques were employed to measure the TPA cross-section of materials [27–29].

In order to design and synthesize active compounds with large TPA/TPF activities and to understand the intrinsic mechanisms, a detailed investigation of the excited states is of great importance. In the past years, we investigated the TPA properties and ultrafast dynamics of several compounds [29,30].

* Corresponding author. Tel.: +86 21 65642084; fax: +86 21 65641344.
** Corresponding author. Tel.: +86 20 87114346 15, fax: +86 20 87110606.
E-mail addresses: sxqian@fudan.ac.cn (S. Qian), xuhuizhu@scut.edu.cn (X.-h. Zhu).

0143-7208/$ – see front matter © 2011 Published by Elsevier Ltd.
doi:10.1016/j.dyepig.2011.06.032

In this work, we report on the interesting TPA and TPF properties of a new 2,1,3-benzothiadiazole-based red emitter (**Z**) consisting of a D–A–D molecular structure (Fig. 1a). The *n*-octyl moieties at the 9,9-positions of the fluorenyl groups are used to improve the solubility of the resulting compound. The branched molecular structure could be useful to reduce intermolecular interaction at a high solution concentration for instance in TPF measurements, thus improving the fluorescence yield.

2. Material and experimental section

2.1. Synthesis

Compound **Z** was readily synthesized by reaction of the Suzuki reagent **3** [31] with 4,7-bis(5-bromothiophen-2-yl)-2,1,3-benzothiadiazole **4** via a conventional Suzuki coupling reaction (Scheme 1). The ^{1}H NMR spectrum was shown in Fig. 1b.

2.1.1. 3,6-Bis(2-naphthyl)carbazole (*1*)

$Pd(PPh_3)_4$ (224 mg, 0.19 mmol) was added to a mixture of 2-naphthylboronic acid (4.44 g, 25.8 mmol), 3,6-dibromocarbazole (4 g, 12.3 mmol) in toluene (130 mL), aqueous Na_2CO_3 (2 M, 52 mL) and ethanol (26 mL) under a nitrogen atmosphere. The reaction was heated to reflux at 90 °C for 24 h. After being cooled to room temperature, the mixture was diluted with distilled water. The organic layer was separated, dried over anhydrous $MgSO_4$, filtered and concentrated under reduced pressure. The residue was purified by column chromatography with petroleum ether/dichloromethane (3:1) to afford a white solid after washing in ethanol under reflux. Yield: 4.7 g (91%). TLC R_f (3:1 petroleum ether/dichloromethane v/v): 0.34. ^{1}H NMR (300 MHz, $CDCl_3$) δ (ppm): 7.46–7.56 (m, 6H), 7.82–89.00 (m, 10H), 8.13–8.18 (m, 3H), 8.55 (m, 2H). m.p. = 265.4 °C. T_d = >400 °C (with 5% loss). IR (KBr): 3420 cm^{-1} (N–H stretch), 3046 cm^{-1} (=C–H stretch), 1602, 1493 cm^{-1} (–C=C– stretch).

2.1.2. 9-(2-Bromo-9,9-dioctylfluoren-7-yl)-3,6-bis(2-naphthyl) carbazole (*2*)

A mixture of CuI (0.12 g, 0.67 mmol), 18-Crown-6 (0.058 g, 0.22 mmol), K_2CO_3 (1.84 g, 13.36 mmol), 1,3-dimethyl-3,4,5,6-tetrahydro-2(1*H*)-pyrimidinone (DMPU) (2 mL), 2,7-dibromo- 9,9-dioctylfluorene (5.4 g, 10.1 mmol) and compound **1** (2.8 g,

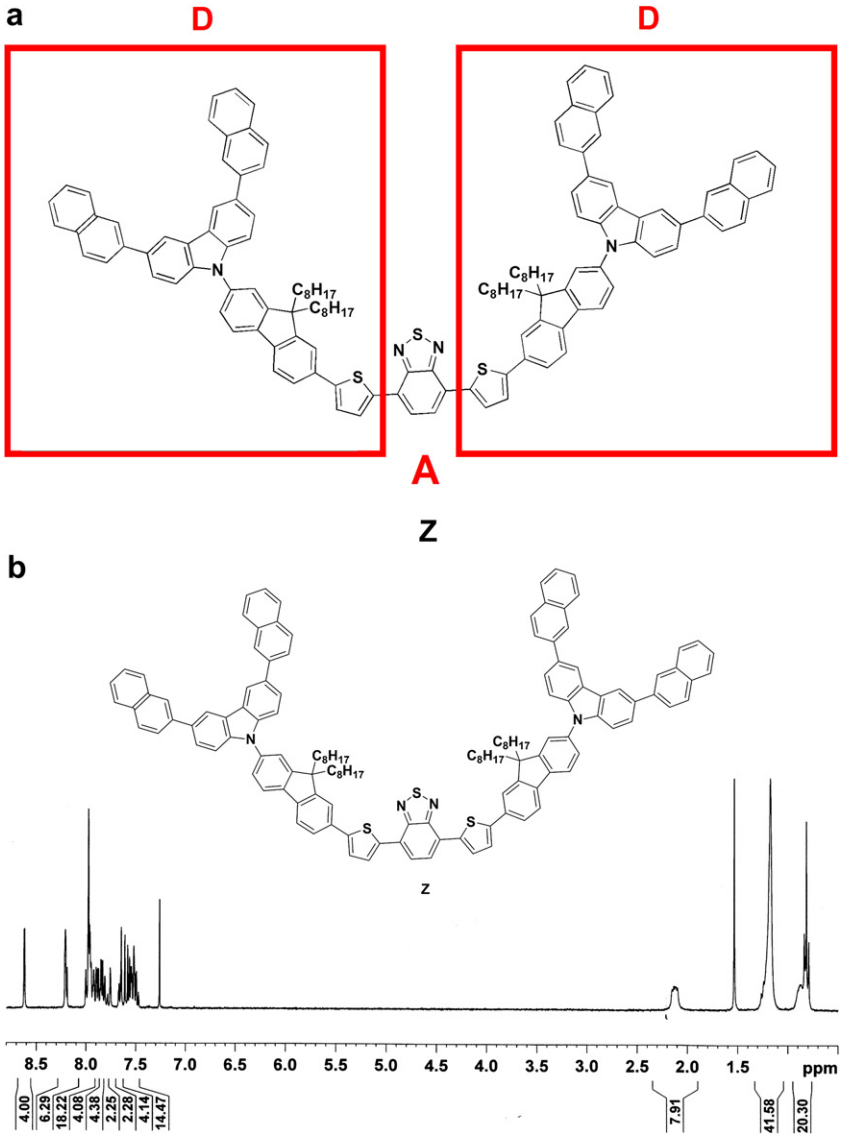

Fig. 1. a) Molecular structure of compound **Z**; b) ^{1}H NMR spectrum.

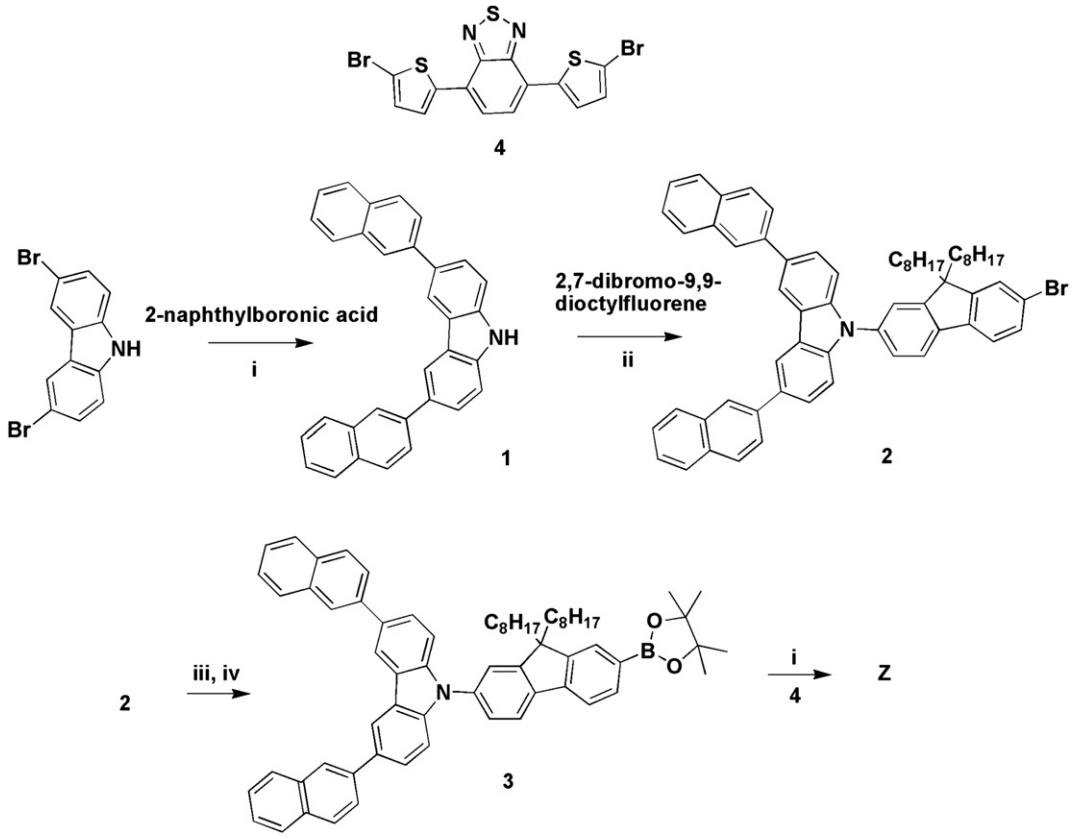

Scheme 1. Synthetic route to compound **Z**. i) $Pd(PPh_3)_4$, 2M Na_2CO_3 aqueous solution, toluene, ethanol, reflux; ii) DMPU, 18-crown-6, CuI, K_2CO_3; iii) *n*-BuLi, THF, −78 °C, iv) 2-isopropoxy-4,4,5,5- tetramethyl-1,3,2-dioxaboralane.

6.68 mmol) was heated at 170 °C for 24 h under nitrogen. After being cooled to room temperature, the mixture was quenched with 1*N* HCl and extracted with dichloromethane. The combined organic phase was washed with water, dried over anhydrous $MgSO_4$, filtered and concentrated under reduced pressure. The crude product was purified by column chromatography with petroleum ether/dichloromethane to afford a white solid. Yield: 3.66 g (64%). TLC R_f (6:1 petroleum ether/dichloromethane v/v): 0.32. ^{1}H NMR (300 MHz, $CDCl_3$) δ (ppm): 0.78–0.89 (m, 10H), 1.15–1.27 (m, 20H), 1.99–2.01 (m, 4H), 7.45–8.00 (m, 22H), 8.20 (s, 2H), 8.60 (d, 2H, J = 1.6 Hz). T_d = >220 °C (with 5% loss). IR (KBr): 3044 cm^{-1} (=C–H stretch), 2923, 2851 cm^{-1} ($-CH_2-$, $-CH_3$ stretch), 1487 cm^{-1}(−C=C−).

2.1.3. 7-(3,6-Bis(2-naphthyl)carbazol-9-yl)-9,9-dioctylfluoren-2-ylboronic pinacol ester (**3**)

A solution of *n*-BuLi in hexanes (2.5 M, 2.1 ml, 5.2 mmol) was slowly added to a solution of. compound **2** (3.5 g, 4 mmol) in dry THF (35 mL) at −78 °C under nitrogen. The mixture was stirred for 30 min at this temperature, and then 2-isopropoxy-4,4,5,5-tetramethyl- 1,3,2-dioxaborolane (1.08 mL, 5.2 mmol) was added. The reaction mixture was stirred for 12 h under nitrogen whilst gradually warming to room temperature. A portion of distilled water was added. The organic phase was extracted into dichloromethane, dried over anhydrous $MgSO_4$, filtered and concentrated under reduced pressure. The residue was purified by silica chromatography using petroleum ether/dichloromethane (4:1 v/v) as the eluent to afford a white solid. Yield: 2.98 g (81%). TLC R_f (4:1 petroleum ether/dichloromethane v/v): 0.52. ^{1}H NMR (300 MHz, $CDCl_3$) δ (ppm): 0.76–0.91 (m, 10H), 1.01–1.27 (m, 20H), 1.42 (s, 12H), 2.02–2.19 (m, 4H), 7.48–8.01 (m, 22H), 8.20 (s, 2H), 8.60 (d, 2H).

2.1.4. Compound **Z**

Synthesized from compound **3** and 4,7-bis(5-bromothiophen-2-yl)-2,1,3-benzothiadiazole (**4**) according to the procedure described for **1**. TLC R_f (4:1 petroleum ether/dichloromethane v/v): 0.23. ^{1}H NMR (300 MHz, $CDCl_3$) δ (ppm): 0.8–0.93 (m, 20H), 1.1–1.26 (m, 40H), 2.10–2.15 (m, 8H), 7.47–8.00 (m, 48H), 8.19–8.21 (m, 6H), 8.61–8.62 (m, 4H). Elemental analysis (%) calcd. for $C_{136}H_{126}N_4S_3$: C, 85.40; H, 6.64; N, 2.93; S, 5.03. found: C, 85.00; H, 6.66; N, 2.62; S, 4.94. T_g = 116 °C (observed in the first heating run), m.p. = 250 °C. IR (KBr): 3051 cm^{-1}(=C–H stretch), 2923, 2851 cm^{-1} ($-CH_2-$, $-CH_3$ stretch), 1474 cm^{-1}(−C=C−).

2.2. Experimental methods

The UV–visible absorption spectra of compound **Z** in tetrahydrofuran (THF) and in the solid state were obtained on a HP 8453 spectrophotometer. One-photon fluorescence spectra were measured by using a Jobin–Yvon spectrofluorometer JY Fluorolog-3 spectrofluorometer.

The TPA spectrum was obtained by using the TPF method with Rhodamine B as the reference [32]. The ultrafast dynamics were measured by using a femtosecond (fs) pump-probe technique which was described in the previous work [33,34]. The TPF spectra were recorded by a fiber spectrometer (TRISTAN). Femtosecond pulses employed for TPA measurement were generated by a mode-locked Ti-sapphire laser system (OPA, Spectra-physics), with the repetition rate of 1 kHz, the pulse duration of 150 fs, and the wavelength from 650 nm to 810 nm. Pulses employed for ultrafast dynamics measurements were generated by spitfire stage of a fs system, with 140 fs pulse duration, 1 kHz repetition rate and about

300 mW average output power. All the measurements were carried out at room temperature.

3. Results and discussions

3.1. Linear absorption and one-photon fluorescence spectra

The linear absorption spectra and one-photon fluorescence emission spectra of compound **Z** in THF solution and in the solid state are shown in Fig. 2. The solid state film on quartz was spin-cast from tolunene solution [31]. The relevant properties are summarized in Table 1. When dissolved in THF solution (ca. 10^{-5} mol L^{-1}), the absorption band at 515 nm could be attributed to the charge-transfer transition between the terminal electron-donor moieties and the central electron-accepting 2,1,3-benzothiadiazole core [11]. The emission peak is at 625 nm. However, the absorption and emission maxima are red-shifted to 530 nm and 671 nm in the solid film, respectively, which could be caused by the increased intermolecular interaction and the structural rigidification of the chromorphore molecule [19,35].

3.2. Two-photon fluorescence and two-photon cross-section

Compound **Z** emits intense red up-conversion fluorescence under the excitation of fs pulses at wavelength of 800 nm. Fig. 3a shows the fluorescence spectra of compound **Z** in THF solution under different excitation power densities of fs pulses, the inset being the fluorescence intensity versus the square of the excitation power density, confirming that the strong fluorescence emission is indeed generated by the TPA process. It should be noticed that, the TPF spectrum of compound **Z** features two emission peaks. The shorter wavelength peak located at 477 nm should be attributed to the transition from the first excited state S_1 to the ground state S_0. The longer emission peak located at 645 nm shows a 20 nm red-shift in comparison to that in one-photon fluorescence spectrum. This red shift would be attributed to the reabsorption effect [36], as we used a much higher concentration (0.01 M) of **Z** in the TPF measurement than that used in one-photon experiment.

The fluorescence quantum yield was determined to be 0.36 in THF solution using Rhodamine B as reference ($\Phi = 0.64$ in ethanol, excited at 510 nm), similar to those of the analogue emitters reported earlier [31]. We measured the TPA cross-section of compound **Z** determined by the TPF method uses fs pulses at 650–810 nm with Rhodamine B in ethanol as the reference. The

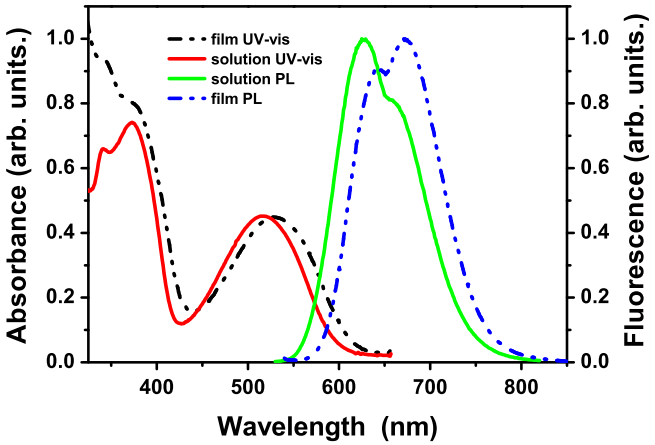

Fig. 2. The linear absorption and steady-state fluorescence spectra of compound **Z**, including the solution in THF solution and thin film.

Table 1
Optical properties of compound **Z** in THF solution and as film.

λ_{abs}[a] (nm)	λ_{flu}[b] (nm)	Δs[c] (nm)	ϕ[d]	λ_{TPE}[e] (nm)	σ_{810}[f] (GM)	σ_{max}[g] (GM)
340/373/515 (solution)	625	90	0.36	477/645	310	2103
342/374/530 (solid)	671	141				

[a] Peak wavelengths of absorption spectra.
[b] The peak wavelength of one-photon fluorescence.
[c] Stokes shift are calculated from the absorption and one photon fluorescence spectra.
[d] Fluorescence quantum yield measured in THF.
[e] The peak wavelength of fluorescence by two-photon exciting.
[f] TPA cross section measured by TPF methods at wavelength of 810 nm.
[g] Peak two-photon absorptivity in GM (10^{-50} cm^4 s photon^{-1}).

TPA cross-section of sample can be calculated by Equation (1), in which the subscripts s and r stand for the sample and reference compound, respectively.

$$\sigma_s = \sigma_r(S_s/S_r)(\Phi_r/\Phi_s)(\phi_r/\phi_s)(c_r/c_s) \quad (1)$$

S is the integral area of the detected two-photon induced fluorescence signal, Φ is the fluorescence quantum yield. ϕ is the overall fluorescence collection efficiency, c is the molar concentration. In the measurement, the collection efficiencies of sample and reference compounds were nearly the same. The two-photon fluorescence excitation spectrum of compound **Z** is shown in Fig. 3b. The TPA cross-section at wavelength of 810 nm was determined to be 310 GM. When the wavelength was tuned to shorter wavelength, the value of the TPA cross-section increased gradually. The TPA cross-section at 650 nm was measured to be 2103 GM. Due to the wavelength limitation of the fs laser system, we cannot measure the values at the region shorter than 650 nm. Even though, the measured value of the TPA cross-section of our compound at 650 nm is much larger than those of 2,1,3-benzothiadiazole based derivatives reported recently in literature [10–12], indicating that our molecular design for the improvement of the TPF property is effective.

3.3. Ultrafast excited state dynamics

In order to investigate the excited state relaxation process as well as the nature of the ICT properties, a femtosecond pump-probe experiment was carried out. A portion of the 800 nm laser beam was used to generate a white-light supercontinuum to provide the probe pulses, another portion was frequency-doubled to 400 nm by a 0.5 mm thick beta-barium borate crystal to generate pump pulses.

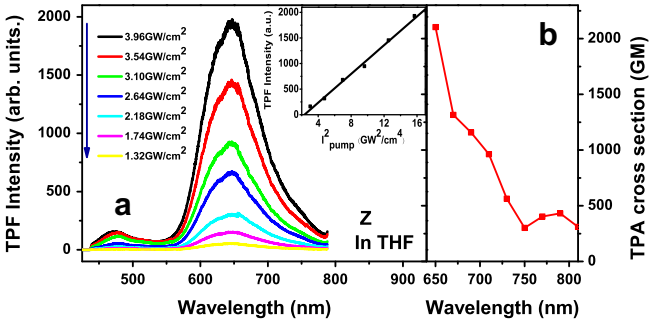

Fig. 3. a) TPF spectra of compound **Z** under different excitation power densities. Inset is TPF intensity versus the square of the excitation power density. b) Two-photon absorption spectrum of compound **Z** in 650–810 nm region.

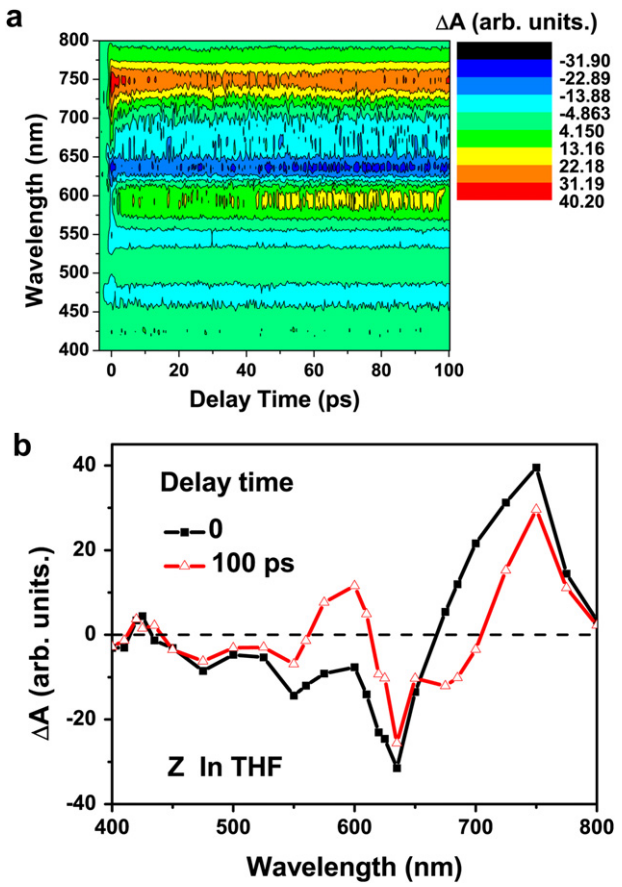

Fig. 4. a) The evolution of fs transient absorption spectra of compound **Z** in THF solution pumped by 400 nm pulses; b) transient absorption spectra at time delays of 0 ps and 100 ps between pump and probe pulse.

The polarization of the pump beam was set to be perpendicular with respect to that of the probe beam in order to sample pure depopulation dynamics. The evolution of fs transient absorption spectra of compound **Z** in THF solution pumped by 400 nm pulses is shown in Fig. 4a, and the transient absorption spectra at time delays of 0 ps and 100 ps between pump and probe pulse are shown in Fig. 4b.

At an initial time delay of 0 ps, a transient photobleaching region around 450–675 nm and a transient photoabsorption region beyond 675 nm are observed. The photoabsorption region is attributed to the absorption of the excited state, and the photobleaching region is mainly caused by stimulated emission of fluorescence. At the delay time of 100 ps, in the wavelength regions of 45–575 nm, 625–700 nm and below 425 nm, the compound shows photobleaching behavior, whereas a photoabsorption signal is observed in the other wavelength regions, for instance, between 575 and 625 nm.

Fig. 5 shows the decay traces at several representative probe wavelengths. The calculated time constants are summarized in Table 2. Very different decay properties were observed at different probe wavelengths. At a wavelength of 400 nm, the dynamics of compound **Z** is dominated by a very long photoabsorption process. When the probe wavelength was tuned to 435 nm, a weak bleaching peak emerged, together with a long (>1000 ps) and relatively weak photoabsorption component. When the probe pulses were tuned to even longer wavelength, the photobleaching peak was firstly strengthened, and finally evolved into a sharp photoabsorption peak at wavelength longer than 670 nm. The long process shows a photobleaching feature in wavelength range of 450–700 nm (except 560–610 nm). When the probe wavelength was tuned from 700 to 800 nm, the long photoabsorption process of dynamics was strengthened gradually. It has been noted in literature that the rise and decay dynamics of the fluorescence (photobleaching signal) show obvious wavelength

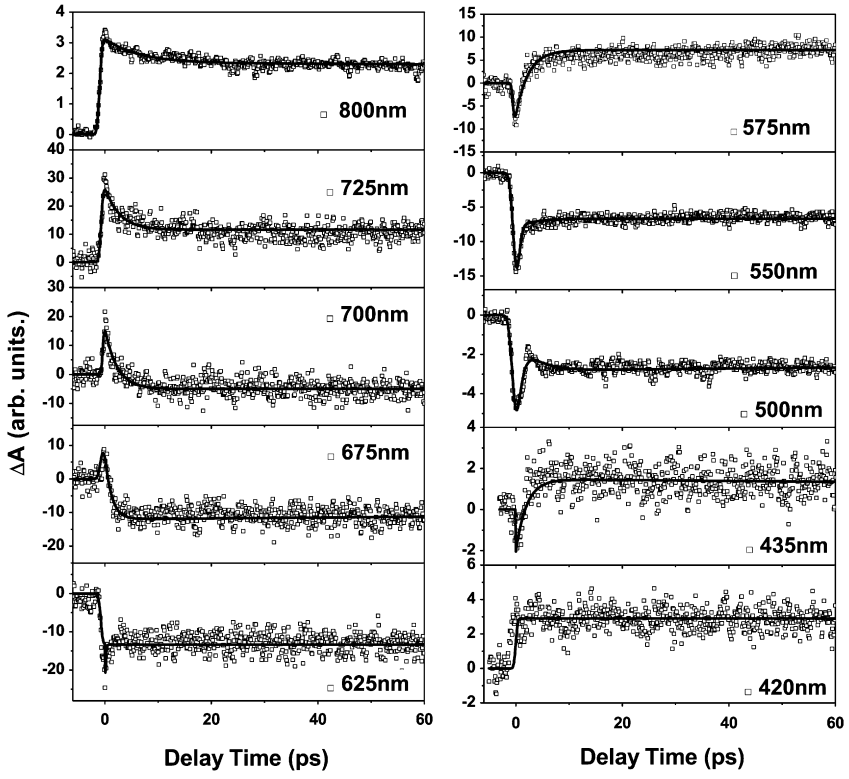

Fig. 5. Dynamics decay traces for compound **Z** in THF at different probe wavelengths.

Table 2
Summary of the time constants of compound **Z** in THF solution.

$\lambda_{Pump/probe}$/nm	Decay/ps	
	τ_1/ps	τ_2/ps
400/420	>1000	/
400/550	1.3	>1000
400/625	0.5	>1000
400/725	2.1	>1000
400/800	4.2	>1000

dependence [37,38]. Thus, the detected dynamics traces could be ascribed to the competition between the pure excited state relaxation and stimulated radiation, resulting in the observed fast component. The long decay component with a time constant of over 1000 ps is attributed to the decay of the ICT state which is always accompanied with strong fluorescence emission. The stimulated radiation at the probe wavelength may affect the signal intensity of the long process [30].

4. Conclusions

In conclusion, the new 2,1,3-benzothiadiazole–based red fluorescent compound has shown good solubility, high fluorescence quantum yield and a large TPA cross-section. The ultrafast dynamics measured by fs pump-probe technique gives a deep understanding of the energy transfer processes inside the compound under the excitation, and reveal a long relaxation lifetime of the ICT state, which is closely related to the efficient fluorescence emission of this compound. The nonlinear fluorescence investigation further shows that this compound has superior properties in TPF emission with a high yield, indicating that for this benzothiadiazole based D–A–D structure, two-photon absorption is an effective excitation route. The compound reported here shows high potential for two-photon fluorescence-based imaging applications.

Acknowledgement

We gratefully thank the financial support (Grant Nos. 60978055, 10674031, 2009ZM0300 & 2009CB930604). The Program for a Special Professorship Appointment (Eastern Scholar) at Shanghai Institutions of Higher Learning. Science and Technology Commission of Shanghai Municipal (09530501100).

References

[1] He GS, Xu GC, Prasad PN, Reinhardt BA, Bhatt JC, Dillard AG. 2-Photon absorption and optical-limiting properties of novel organic-compounds. Optics Letters 1995;20:435.
[2] Kasischke KA, Vishwasrao HD, Fisher PJ, Zipfel WR, Webb WW. Neural activity triggers neuronal oxidative metabolism followed by astrocytic glycolysis. Science 2004;305:99–103.
[3] Kawata S, Sun HB, Tanaka T, Takada K. Finer features for functional microdevices – micromachines can be created with higher resolution using two-photon absorption. Nature 2001;412:697–8.
[4] Cumpston BH, Ananthavel SP, Barlow S, Dyer DL, Ehrlich JE, Erskine LL, et al. Two-photon polymerization initiators for three-dimensional optical data storage and microfabrication. Nature 1999;398:51–4.
[5] Zhao CF, Gvishi R, Narang U, Ruland G, Prasad PN. Structures, spectra, and lasing properties of new (aminostyryl)pyridinium laser dyes. Journal of Physical Chemistry 1997;100:4526–32.
[6] Bhawalkar JD, He GS, Park CK, Zhao CF, Ruland G, Prasad PN. Efficient, two-photon pumped green upconverted cavity lasing in a new dye. Optics Communications 1996;124:33–7.
[7] Denk W, Strickler JH, Webb WW. 2-Photon laser scanning fluorescence microscopy. Science 1990;248:73–6.
[8] Brousmiche DW, Serin JM, Fréchet JMJ, He GS, Lin TC, Chung SJ, et al. Fluorescence resonance energy transfer in novel multiphoton absorbing dendritic structures. Journal of Physics Chemistry B 2004;108:8592–600.
[9] Margineanu A, Hofkens J, Cotlet M, Habuchi S, Stefan A, Qu JQ, et al. Photophysics of a water-soluble rylene dye: comparison with other fluorescent molecules for biological applications. Journal of Physical Chemistry B 2004;108:12242–51.
[10] Kato S, Matsumoto T, Ishi-I T, Thiemann T, Shigeiwa M, Gorohmaru H, et al. Strongly red-fluorescent novel donor-π-bridge-acceptor-pi-bridge-donor (D-π-A-π-D) type 2,1,3-benzothiadiazoles with enhanced two-photon absorption cross-sections. Chemical Communications 2004;20:2342–3.
[11] Kato S, Matsumoto T, Shigeiwa M, Gorohmaru H, Maeda S, Ishi-I T, et al. Novel 2,1,3-benzothiadiazole-based red-fluorescent dyes with enhanced two-photon absorption cross-sections. Chemistry-A European Journal 2006;12:2303–17.
[12] Tian YQ, Wu WC, Chen CY, Strovas T, Li YZ, Jin YG, et al. 2,1,3-Benzothiadiazole (BTD)-moiety-containing red emitter conjugated amphiphilic poly(ethylene glycol)-block-poly(epsilon-caprolactone) copolymers for bioimaging. Journal of Materials Chemistry 2010;20:1728–36.
[13] Weissleder R. A clearer vision for in vivo imaging. Nature Biotechnology 2001;19:316–7.
[14] Graves EE, Weissleder R, Ntziachristos V. Fluorescence molecular imaging of small animal tumor models. Current Molecular Medicine 2004;4:419–30.
[15] Kitamura C, Tanaka S, Yamashita Y. Design of narrow-bandgap polymers. Syntheses and properties of monomers and polymers containing aromatic-donor and o-quinoid-acceptor units. Chemistry of Materials 1996;8:570–8.
[16] Raimundo J-M, Blanchard P, Brisset H, Akoudad S, Roncali J. Proquinoid acceptors as building blocks for the design of efficient π-conjugated fluorophores with high electron affinity. Chemical Communications 2000;11:939–40.
[17] Justin Thomas KR, Lin JT, Velusamy M, Tao Y-T, Chuen C-H. Color tuning in benzo[1,2,5]thiadiazole-based small molecules by amino conjugation/deconjugation: bright red-light-emitting diodes. Advanced Functional Materials 2004;14:83–90.
[18] Huang J, Qiao XF, Xia YJ, Zhu XH, Ma DG, Cao Y, et al. A Dithienylbenzothiadiazole pure red molecular emitter with electron transport and exciton self-confinement for nondoped organic red-light-emitting diodes. Advanced Materials 2008;20:4172.
[19] Huang J, Liu Q, Zou JH, Zhu XH, Li AY, Li JW, et al. Electroluminescence and laser emission of soluble pure red fluorescent molecular glasses based on dithienylbenzothiadiazole. Advanced Functional Materials 2009;19:2978–86.
[20] Li Y, Li AY, Li BX, Huang J, Zhao L, Wang BZ, et al. Asymmetrically 4,7-disubstituted benzothiadiazoles as efficient non-doped solution-processable green fluorescent emitters. Organic Letters 2009;11:5318–21.
[21] Shen M, Rodriguez Lopez J, Huang J, Liu Q, Zhu XH, Bard AJ. Electrochemistry and electrogenerated chemiluminescence of dithienylbenzothiadiazole derivative. Differential reactivity of donor and acceptor groups and simulations of radical cation–anion and dication-radical anion annihilations. Journal of American Chemical Society 2010;132:13453–61.
[22] Zhang J, Yang Y, He C, He Y-J, Zhao G-J, Li Y-F. Solution-processable star-shaped photovoltaic organic molecule with triphenylamine core and benzothiadiazole-thiophene arms. Macromolecules 2009;42:7619–22.
[23] He GS, Tan L-S, Zheng QD, Prasad PN. Multiphoton absorbing materials: molecular designs, characterizations, and applications. Chemical Reviews 2008;108:1245–330.
[24] Rumi M, Barlow S, Wang J, Perry JW, Marder SR. Two-photon absorbing materials and two-photon-induced chemistry. Advances in Polymer Science 2008;213:1–95.
[25] Bhaskar A, Ramakrishna G, Lu ZK, Twieg R, Hales JM, Hagan DJ, et al. Investigation of two-photon absorption properties in branched alkene and alkyne chromophores. Journal of American Chemical Society 2006;128:11840–9.
[26] Gu B, Ji W, Patil PS, Dharmaprakash SM. Ultrafast optical nonlinearities and figures of merit in acceptor-substituted 3,4,5-trimethoxy chalcone derivatives: structure-property relationships. Journal of Applied Physics 2008;103:103511.
[27] Sahraoui B, Kityk IV, Fuks I, Paci B, Baldeck P, Nunzi JM, et al. Novel nonlinear optical organic materials: dithienylethylenes. Journal of Chemical Physics 2001;115:6179–84.
[28] Anémian R, Morel Y, Baldeck PL, Paci B, Kretsch K, Nunzi JM, et al. Optical limiting in the visible range: molecular engineering around N4, N4′-bis(4-methoxyphenyl)-N4, N4′-diphenyl- 4,4′-diaminobiphenyl. Journal of Material Chemistry 2003;13:2157–63.
[29] Li B, Tong R, Zhu R, Meng F, Tian H, Qian S. The ultrafast dynamics and nonlinear optical properties of tribranched styryl derivatives based on 1,3,5-triazine. Journal of Physical Chemistry B 2005;109:10705–10.
[30] Wang YC, Zhang DK, Zhou H, Ding JL, Chen Q, Xiao Y, et al. Nonlinear optical properties and ultrafast dynamics of three novel boradiazaindacene derivatives. Journal of Applied Physics 2010;108:033520.
[31] Huang J, Li J, Xia YJ, Zhu XH, Peng JB, Cao Y. Amorphous fluorescent organic emitters for efficient solutiion-processed pure red electroluminescence: synthesis, purification, morphology, solid-state photoluminescence, and device characterizations. Journal of Organic Chemistry 2007;72:8580–3.
[32] Oulianov DA, Tomov IV, Dvornikov AS, Rentzepis PM. Observations on the measurement of two-photon absorption cross-section. Optics Communications 2001;191:235–43.
[33] Mi J, Guo LJ, Liu Y, Liu WM, You GJ, Qian SX. Excited-state dynamics of magnesium phthalocyanine thin film. Physics Letters A 2003;310:486–92.

[34] Sheik-Bahae M, Said AA, Wei TH, Hagan DJ, Vanstryland EW. Sensitive measurement of optical nonlinearities using a single beam. IEEE Journal of Quantum Electronics 1990;26:760–9.
[35] Xia RD, Heliotis G, Hou YB, Bradley DDC. Fluorene-based conjugated polymer optical gain media. Organic Electronics 2003;4:165–77.
[36] Wu LZ, Tang XJ, Jiang MH, Tung CH. Two-photon induced fluorescence of novel dyes. Chemical Physics Letters 1999;315:379–82.
[37] Yan YL, Li B, Liu KJ, Dong ZW, Wang XM, Qian SX. Enhanced two-photon absorption and ultrafast dynamics of a new multibranched chromophore with a dibenzothiophene core. Journal of Physical Chemistry A 2007;111:4188–94.
[38] Toele P, Van Gorp JJ, Glasbeek M. Femtosecond fluorescence studies of self-assembled helical aggregates in solution. Journal of Physical Chemistry A 2005;109:10479–87.